Use Of High Modulus Carbon Fiber Reinforced Polymers(CFRP) For Strengthening of Steel Columns

Rana F. Yousif
University of Babylon - College of Engineering - civil Engineering Department

Abstract

The experimental research reported is aimed using small quantities of CFRP strips to provide against web or/and flange local buckling for (8) specimens of steel columns . Steel columns with (I) section specimens are made from welding thin plates at their edges between web and flange . The type of strengthen carbon fiber is a unidirectional woven fiber mat of mid strength which is a product of Sika coded as SikaWrap-230C. The CFRP is fixed using a resin Sikadure-330.The study is focusing on the local stability of such members. Many pattern of wrapping are suggested herein. Recommendations have been drawn for the best pattern chosen to obtain the most efficient and economic strengthen pattern. This technique has the potential to correct difficulties associated with existing techniques while being cost-effective and causing minimal disruption to the users of the structure. Also formulation of the finite element method used for analyzing the tested columns. The finite element model will be using the experimental load-deflection results of the steel columns. The use of ANSYS-8 to create the finite element model is adopted, the maximum different between experimental results and ANSYS-8 results is 4.8%.

الخلاصة

تم تحري السلوك ألمختبري باستعمال كمية قليلة من شرائح ألياف الكربون البوليمري (CFRP) لتحسين أداء الانحناء الموضعي للويب والحافة لثمان نماذج من الأعمدة الحديدية. تم تصنيع نماذج الأعمدة الحديدية بشكل حرف (I) من لحم صفائح نحيفة الجدران في الحافات ما بين الويب والحافة. نوع التقوية تمت باستعمال حصيرة ألياف كربون منسوجة باتجاه واحد من النوع المتوسط المقاومة إنتاج شركة سيكا ذو الرمز (Sika Wrap-230C). تم تثبيت ألياف الكربون باستعمال راتنج نوع (Sikadure-330). ركزت الدراسة على الاستقرارية الموقعية لمثل هذه الأعضاء. تم اقتراح أنماط عديدة للتقوية.تم استخلاص توصيات لأفضل نمط من ناحية الكفاءة و الاقتصاد. هذه التقنية وفرت إمكانية تذليل الصعوبات المرتبطة بإيجاد تقنية توفر الكلفة والفعالية بأقل ما ممكن من عرقلة للمستخدمين المنشأ.وبطريقة العناصر المحددة تم تحليل الأعمدة المفحوصة مختبريا. وهذه الطريقة اعتمد على النتائج العملية لمنحني الحمل والهطول للأعمدة الحديدية. بالاعتماد على ANSYS-8تم تطبيق طريقة العناصر المحددة وأقصى فرق بين النتائج العملية ونتائج ANSYS-8 كانت 4.8%.

Introduction

Recent research on the strengthening of circular hollow sections (CHS) with FRP by Teng and Hu (2007) and Hong et al. (2000) in axial compression, Haedir et al.(2007,2006) in bending, Doi et al. (2003)in bending and compression, Jiao and zhao (2004) in tension, and Zhao et al (2005) and Xiao et al. (2005) on concrete filled CHS, have shown significant benefits in strength and stiffness of steel members with externally bonded CFRP. Experiments on steel RHS strengthened with CFRP under transverse end bearing force were described by Zhao et al. (2006). The mechanical properties of reinforced fiber rely on the fiber characteristics, such as their size, the percentage of fiber reinforcement, and the orientations of fibers. One of the greatest limitations to the behavior of conventional steel tubular beams composed of thin section is the susceptibility of the steel component to local buckling. This local instability is more likely to occur in thin than in thick section, and the effect of local stresses within the steel can result in a reduction of strength.

Experimental Setup and Test Specimens:

The section dimensions of the specimens produced by seam-welded along length of three parts of steel with 2mm thickness, 120mm length of web, 100mm length of flange and 500mm height of 320Mpa yield steel. The measured uni-axial tensile material properties are listed in Table 1. Fig1 shown section of the specimen, Fig2 Shown the measured uni-axial tension stress-strain material curve of the steel sheets which used to fabricate the tuber steel columns.

Table(1)

The dimension and the measured uni-axial tension material properties of the Steel sheets which used to fabricate the tuber steel columns.

Specimen	Thickness *t (mm)*	Length of flange (mm)w_1	Length of web (mm)w_2	Length l (mm)	Yield Stress f_y (Mpa)	Ultimate Stress f_u (Mpa)	Failure Strain ε_f
1 to 8	2	100	120	500	320	400	0.10714

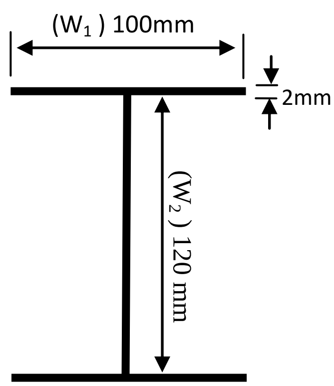

Fig(1) Section of specimen

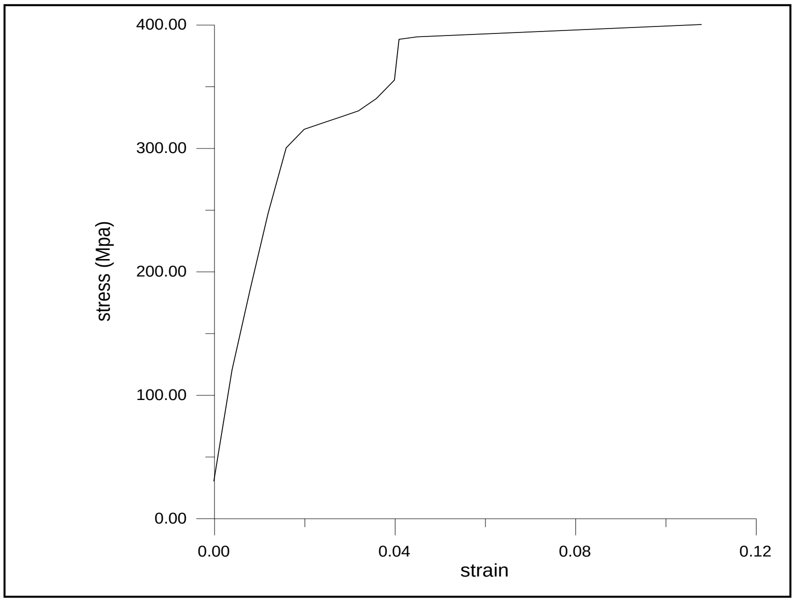

Fig. (2) The measured uni-axial tension stress-strain material curve.

The tuber steel columns strengthen with different of woven carbon fiber type Sika Wrap-230C by epoxy Sikadure-330 the material properties are tabulated in Table 2.

Table(2)
The material properties of Sika Wrap-230c carbon fiber and Sikadure-330 epoxy.

Material	Fabric design Thickness (mm)	Fiber density g/cm^3	Areal weight g/m	Tensile strength (Mpa)	E-Modulus (Mpa)
Sika Wrao-230C	0.131	1.76	230	4300	238000
Sikadure-330	----	----	----	30	4500

The test program include tested eight structure column; non strengthen steel column (NS), columns strengthen with longitudinal CFRP for the two face of the web only by strip with width(2.8cm) was applied with inclination of (45°,63.43° and26.57°)for (PS1), (PS2) and (PS3) respectively.

The column (PS4,PS5 and PS6)have the same distribution of CFRP of column (PS1,PS2 and PS3) but at the two face of the flange. The column (PS7) strengthen with longitudinal CFRP as two strip with (3cm) width at the web but the flange strengthen by CFRP as two strip with (2cm) width.

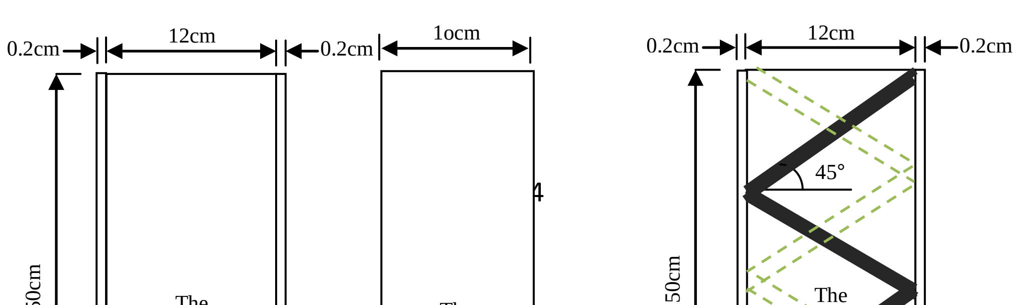

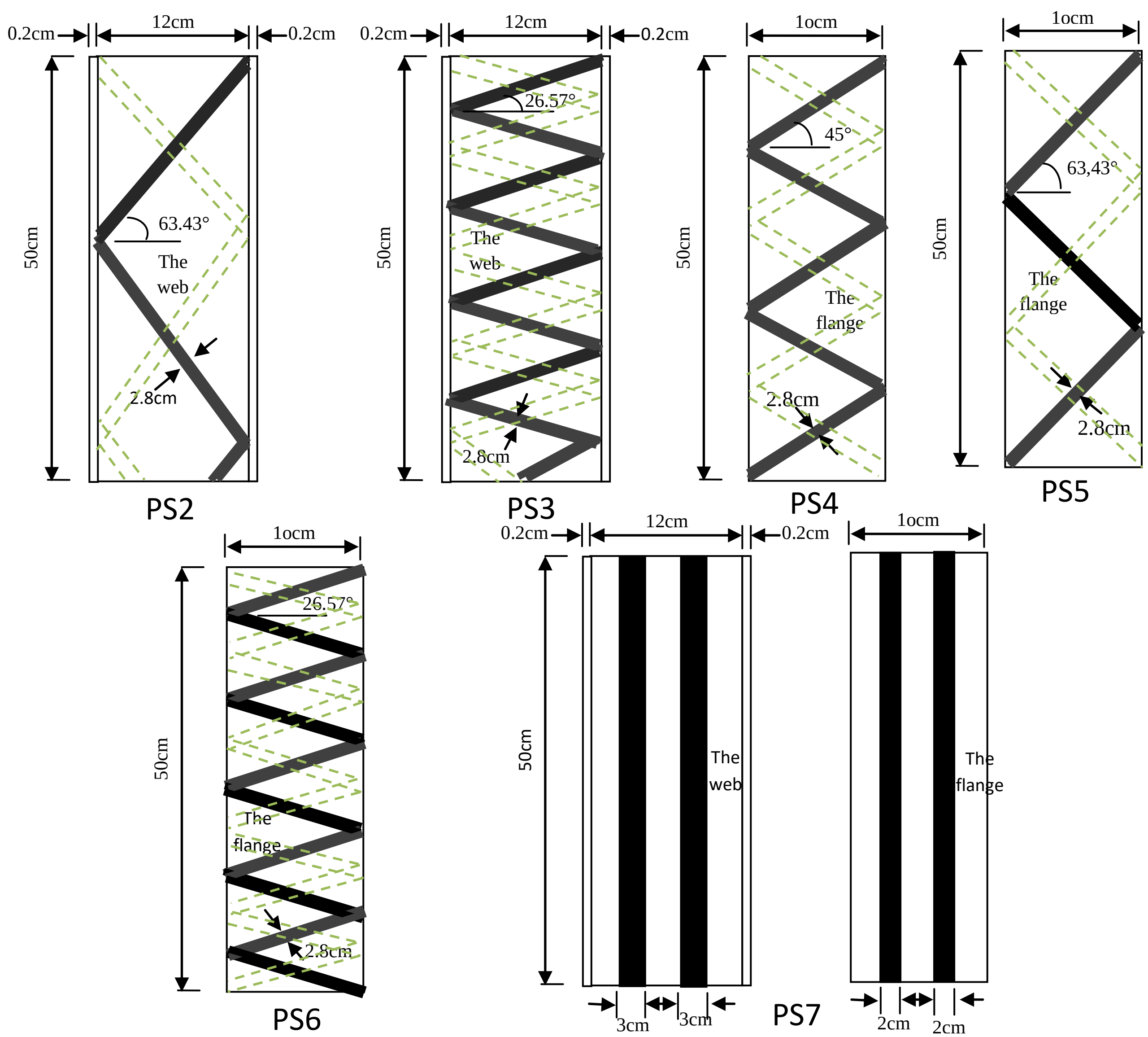

Figure (3) The distribution Pattern of CFRP of the tested specimens

Finite Element Modeling:

General:

The finite element method has become a powerful tool for the numerical solution of a wide range of engineering problems. In this search the formulation of the finite element method used for analyzing the tested columns is introduced. The use of ANSYS-8 to create the finite element model is adopted. All the necessary steps to create the calibrated model are explained in details and the steps taken to generate the analytical load-deflection response of the member are discussed.

Nonlinear Finite Element Analysis for Structures:

Most phenomena in solid mechanics are nonlinear. However in many applications it is convenient and practical to use linear formulation for problems to obtain engineering solutions. On the other hand, some problems definitely require nonlinear analysis if realistic results are to be obtained such as post-yielding and large deflection behavior of structures. Depending on the sources of nonlinearities, the nonlinear problems can be divided into three categories. In brief, these categories are, Problems involving material nonlinearity, Problems involving geometric nonlinearity and Problems involving both materials and geometric nonlinearity.

The present study deals with material nonlinearity in analyzing the tested columns. This is because large deflection behavior of structures. Buckling loads are critical loads where certain types of structures become unstable. Each load has an associated buckled mode shape; this is the shape that the structure assumes in a buckled condition. There are two primary means to perform a buckling analysis:

1. **Eigenvalue**
   Eigenvalue buckling analysis predicts the theoretical buckling strength of an ideal elastic structure. It computes the structural eigenvalues for the given system loading and constraints. This is known as classical Euler buckling analysis. Buckling loads for several configurations are readily available from tabulated solutions. However, in real-life, structural imperfections and nonlinearities prevent most real-world structures from reaching their eigenvalue predicted buckling strength; ie. it over-predicts the expected buckling loads. This method is not recommended for accurate, real-world buckling prediction analysis.
2. **Nonlinear**
   Nonlinear buckling analysis is more accurate than eigenvalue analysis because it employs non-linear, large-deflection, static analysis to predict buckling loads. Its mode of operation is very simple: it gradually increases the applied load until a load level is found whereby the structure becomes unstable (ie. suddenly a very small increase in the load will cause very large deflections). The true non-linear nature of this analysis thus permits the modeling of geometric imperfections, load perturbations, material nonlinearities and gaps. For this type of analysis, note that small off-axis loads are necessary to initiate the desired buckling mode.

Finite Element Representation of steel columns with External CFRP Reinforcement:

In the field of solid mechanics, the finite element method is usually used to find approximate solutions for structures having complicated shapes and /or loading arrangement. The element types for this model are shown in Table (3) . The SOLID45 element was used to model the steel. This element has eight nodes with three degrees of freedom at each node translation in the nodal x, y and z directions the element has plasticity, creep, swelling, stress stiffening, large deflection, and large strain capabilities. A reduced integration option with hourglass control is available.

While Shell41 represents the CFRP strips, SHELL41 is a 3-D element having membrane (in-plane) stiffness but no bending (out-of-plane) stiffness. It is intended for shell structures where bending of the elements is of secondary importance. The element has three degrees of freedom at each node: translations in the nodal x, y, and z directions. The element is defined by four nodes, four thicknesses, a material direction angle and the orthotropic material properties. Orthotropic material directions correspond to the element coordinate directions. The element coordinate system orientation is as described in Coordinate Systems. The element x-axis may be rotated by an angle THETA (in degrees).The element may have variable thickness. The thickness is assumed to vary smoothly over the area of the element, with the thickness input at the four nodes. If the element has a constant thickness, only TK(I) need be input. If the thickness is not constant, all four thicknesses must be input. Parameter needed to define the material models can be founded in Tables(4) .

Materials Properties:

EX is the modulus of elasticity of the concrete and PRXY is the Poisson's ratio. The bilinear model requires the yield stress as well as the hardening modulus of the steel to be defined.

Table (3) Element types for working model.

Material type	ANSYS element
Steel CFRP strips	SOLID45 SHELL41

Table(4) Material models for the calibration model

<table>
<tr><th>Material model number</th><th>Element Type</th><th>Material properties</th><th>Real Constant</th></tr>
<tr><td>1</td><td>SOLID45</td><td>
<table>
<tr><th colspan="2">Linear Isotropic</th></tr>
<tr><td>EX</td><td>200000</td></tr>
<tr><td>PRXY</td><td>0.3</td></tr>
</table>
<table>
<tr><th colspan="2">Bilinear Isotropic</th></tr>
<tr><td>Yield stss</td><td>280</td></tr>
<tr><td>Tang mod</td><td>2000</td></tr>
</table>
</td><td></td></tr>
<tr><td>2</td><td>SHEEL41</td><td>
<table>
<tr><th colspan="2">Linear orthotropic</th></tr>
<tr><td>EX</td><td>230000</td></tr>
<tr><td>EY</td><td>1</td></tr>
<tr><td>EZ</td><td>1</td></tr>
<tr><td>PRXY</td><td>0</td></tr>
<tr><td>PRYZ</td><td>0</td></tr>
<tr><td>PRXZ</td><td>0</td></tr>
<tr><td>GXY</td><td>1</td></tr>
<tr><td>GYZ</td><td>1</td></tr>
<tr><td>GXZ</td><td>1</td></tr>
</table>
</td><td>
<table>
<tr><td>Shell thickness of node J TK(J)</td><td>0.131</td></tr>
<tr><td>node K TK(K)</td><td>0.131</td></tr>
<tr><td>node L TK(L)</td><td>0.131</td></tr>
<tr><td>node I TK(I)</td><td>0.131</td></tr>
<tr><td>Element x-axis rotation theta</td><td>0°,45°, 26.57°, 63.43°</td></tr>
<tr><td>Elastic foundation stiffness</td><td>0</td></tr>
<tr><td>Add mass/unite area</td><td>0</td></tr>
</table>
</td></tr>
</table>

Experimental and ANSYS results:

The results of the tested specimens that obtained from applying an axial compressive load by using an universal testing machine as shown in Fig. (4), shown that the application of CFRP to the steel columns increase the stiffness, the ultimate axial compressive load and decrease the local buckling at the ends of the column. The obtained results from experimental tested and ANSYS-9 were tabulated in Table (5).The axial compressive load to axial displacement curve for the experimental tested columns are shown in Fig.(13), also the curves of experimental tested for each column and by solved this columns by ANSYS-9 are shown in Fig.(5) and Fig.(6), Fig.(7), Fig.(8), Fig.(9), Fig.(10), Fig.(11) and Fig.(12) also this figures show the shape of columns before and after testing. From these figures it`s clear that the distribution of CFRP was for column PS3. Where this pattern gives a behavior better than the behavior of other columns.

Fig. 4 The universal testing machine.

Table (5) The experimental and ANSYS-9 results of the tested column.

Specimen	P_u (KN)	$\frac{Pu - Po}{Po} * 100$	P_A (KN)	$\frac{PA - Pu}{Pu} * 100$
NS	100	0%	102	2%
PS1	130	30%	125	3.8%
PS2	120	20%	118	1.7%
PS3	135	35%	132	2.2%
PS4	113	13%	118	4.4%
PS5	105	5%	110	4.8%
PS6	115	15%	119	3.5%
PS7	115	15%	120	4.3%

Where: **P_u : ultimate axial load (KN) by experimental tested.**

P_o : ultimate axial load of non strength steel column (KN) by experimental tested.

P_A : ultimate axial load (KN) by ANSYS-9 .

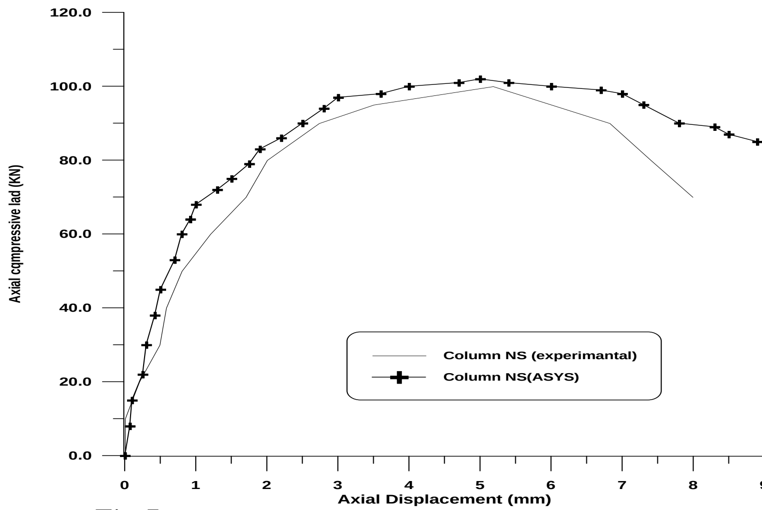


Fig.5 **The axial compressive load to axial displacement curve of column NS by experimental tested and ANSYS -9.**

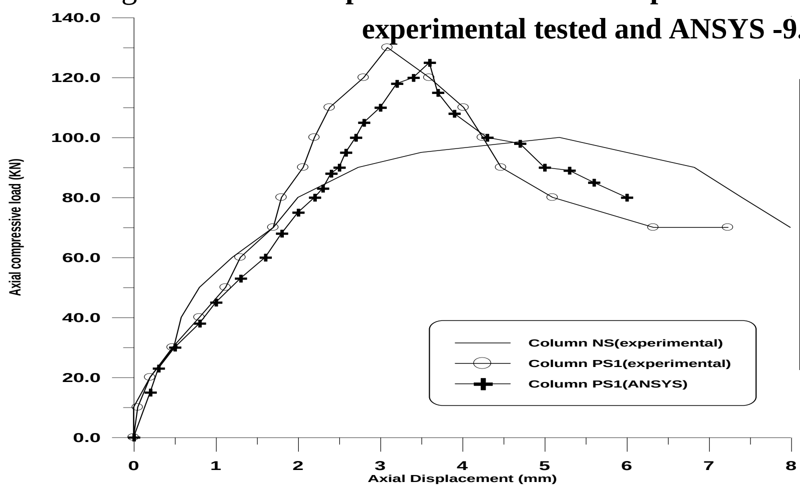


Fig.6 **The axial compressive load to axial displacement curve of column NS and PS1 by experimental tested and ANSYS-9.**

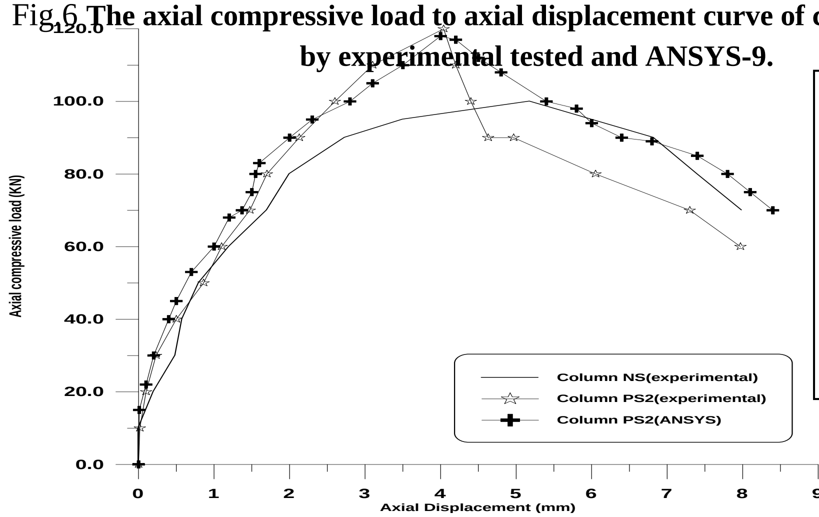


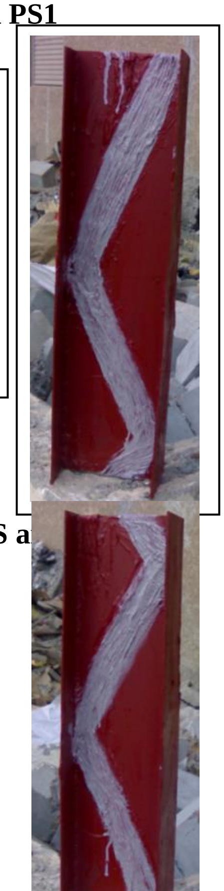

Fig.7 **The axial compressive load to axial displacement curve of column NS a by experimental tested and ANSYS program**

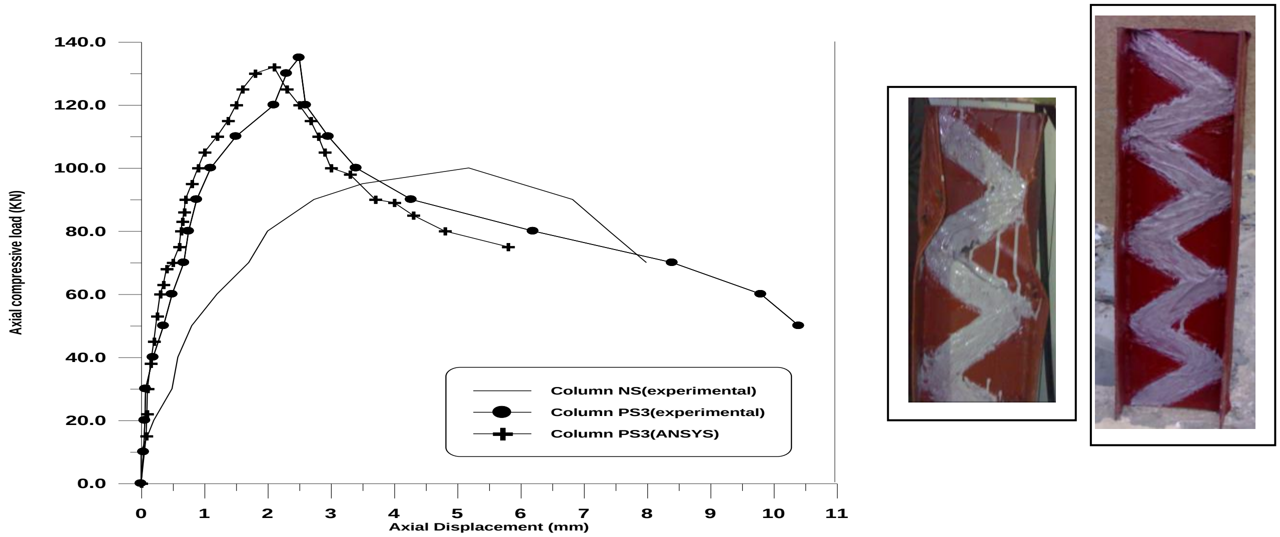

Fig.8 **The axial compressive load to axial displacement curve of column NS and PS3 by experimental tested and ANSYS-9.**

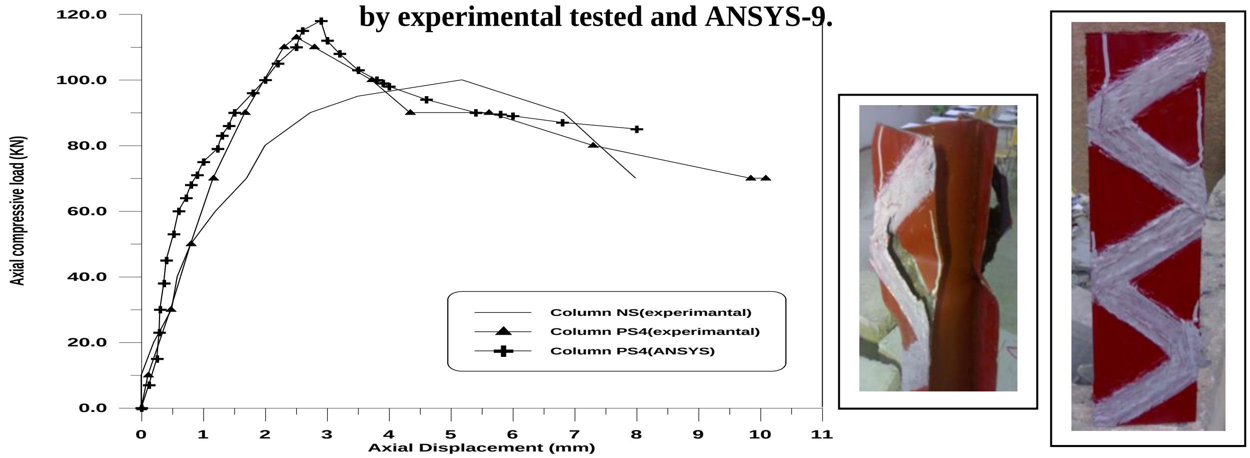

Fig.9 **The axial compressive load to axial displacement curve of column NS and PS4 by experimental tested and ANSYS-9.**

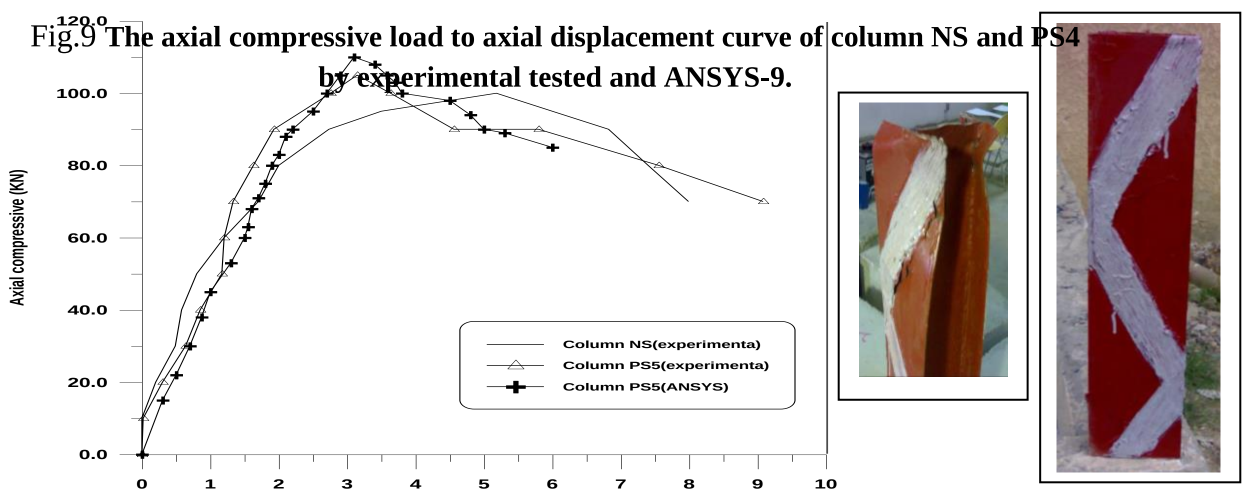

Fig.10 **The axial compressive load to axial displacement curve of column NS and PS5 by experimental tested and ANSYS-9.**

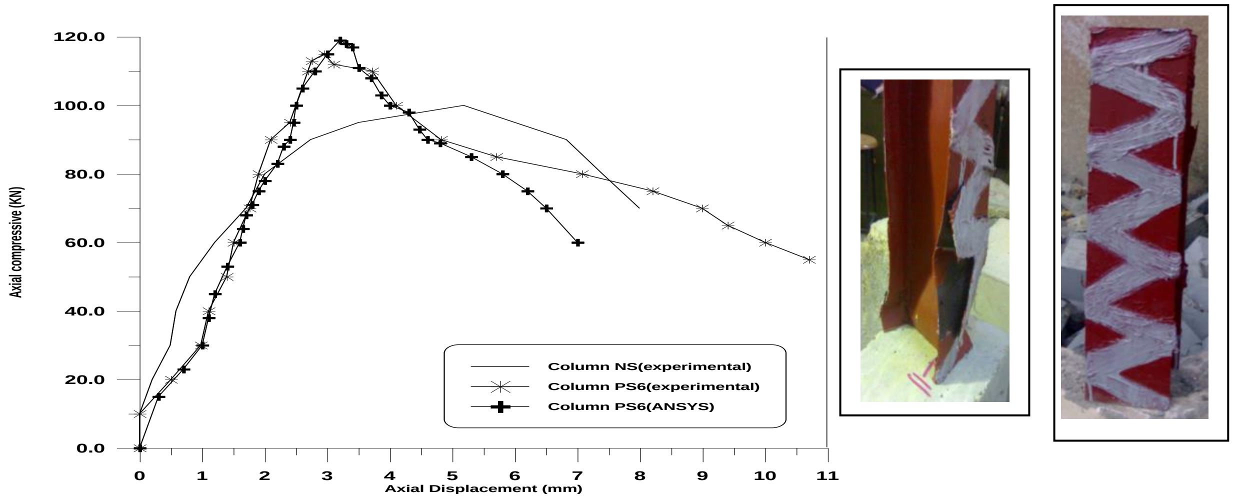

Fig.11 **The axial compressive load to axial displacement curve of column NS and PS6 by experimental tested and ANSYS-9.**

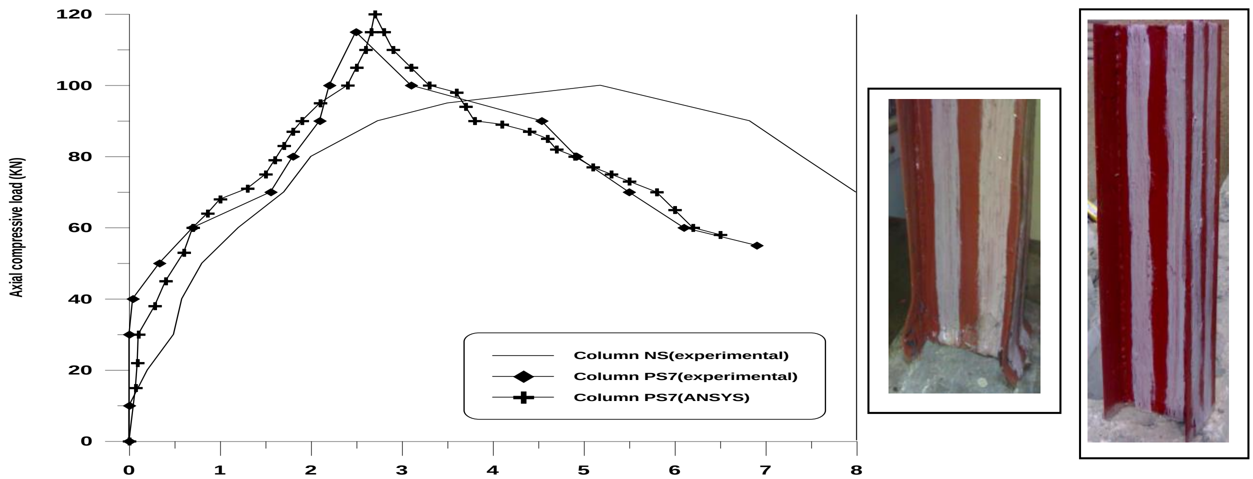

Fig.12 **The axial compressive load to axial displacement curve of column NS and PS7 by experimental tested and ANSYS-9.**

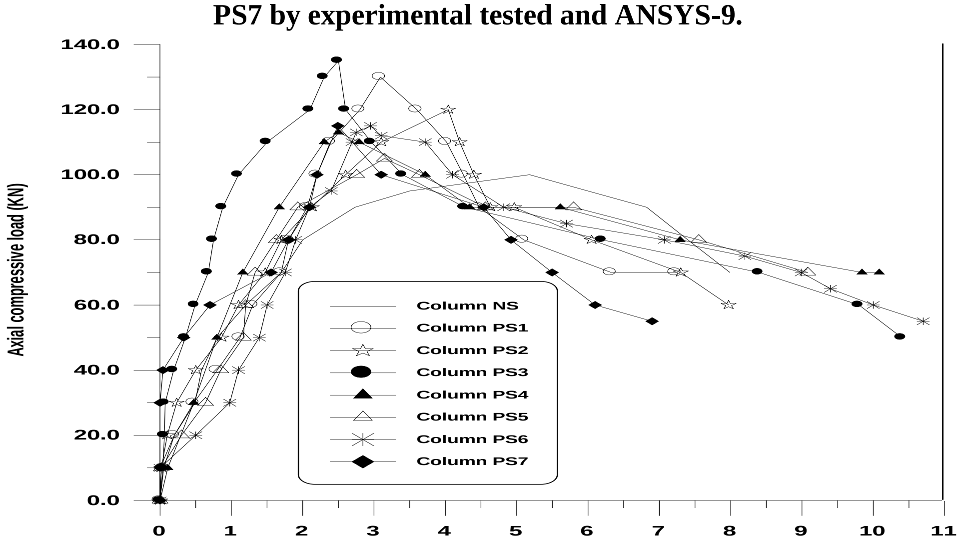

Fig.13 **The experimental axial compressive load to axial displacement curve of the tested columns.**

Fig.14 shows that the column PS3 represented the best distribution of CFRP which increased the ultimate load to about (35%). The columns that strengthened at flange the **CFRP** debonded from the surface happened. The Figures from (16) to (23) show distribution of stresses intensity, Axial displacement in Y direction and distribution of stresses intensity at CFRP of each columns by ANSYS-9 and bulking of NS column shown at Fig.(16).

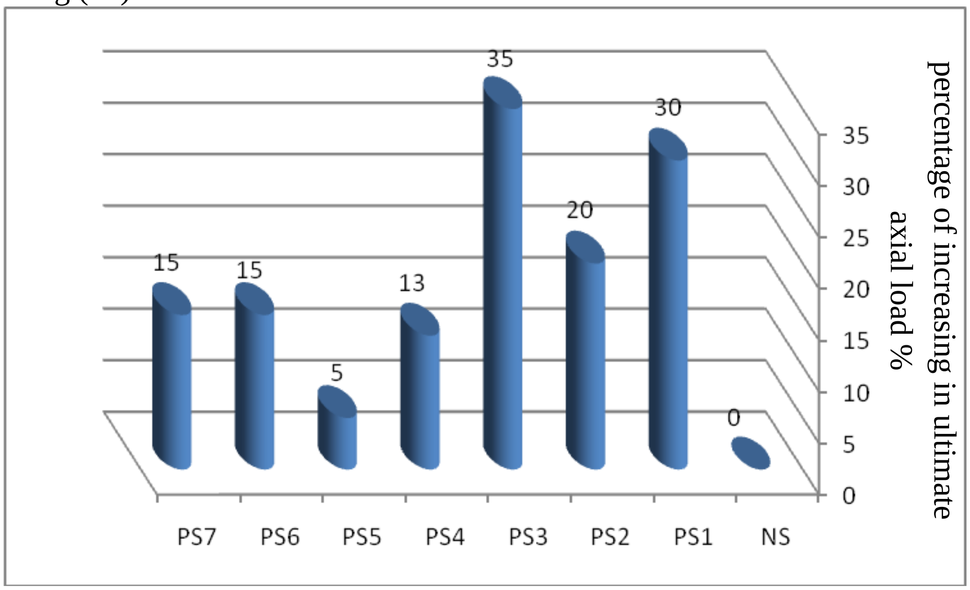

Fig.14 the percentage of increasing to ultimate axial load for the experimental tested columns.

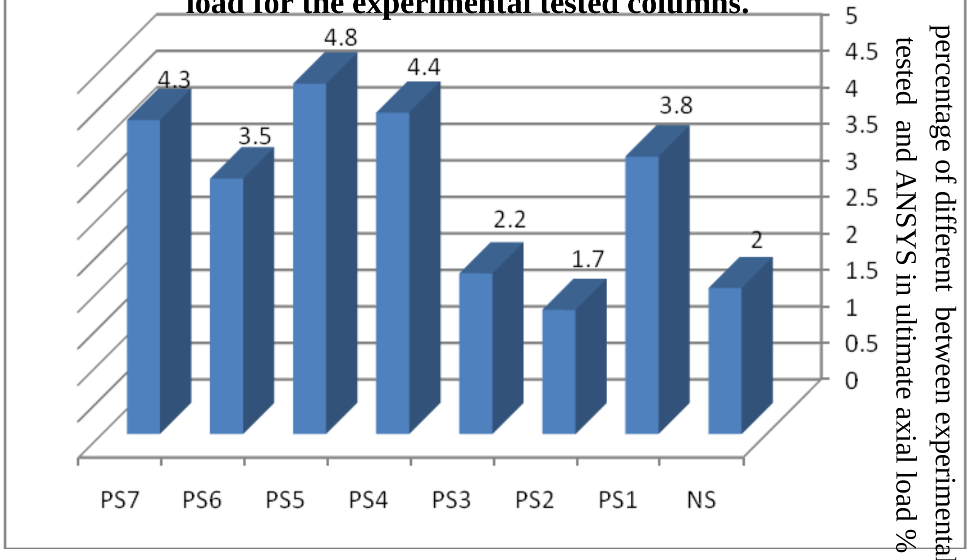

Fig.15 the percentage of difference between ultimate axial load of experimental tested and ANSYS-9 for columns.

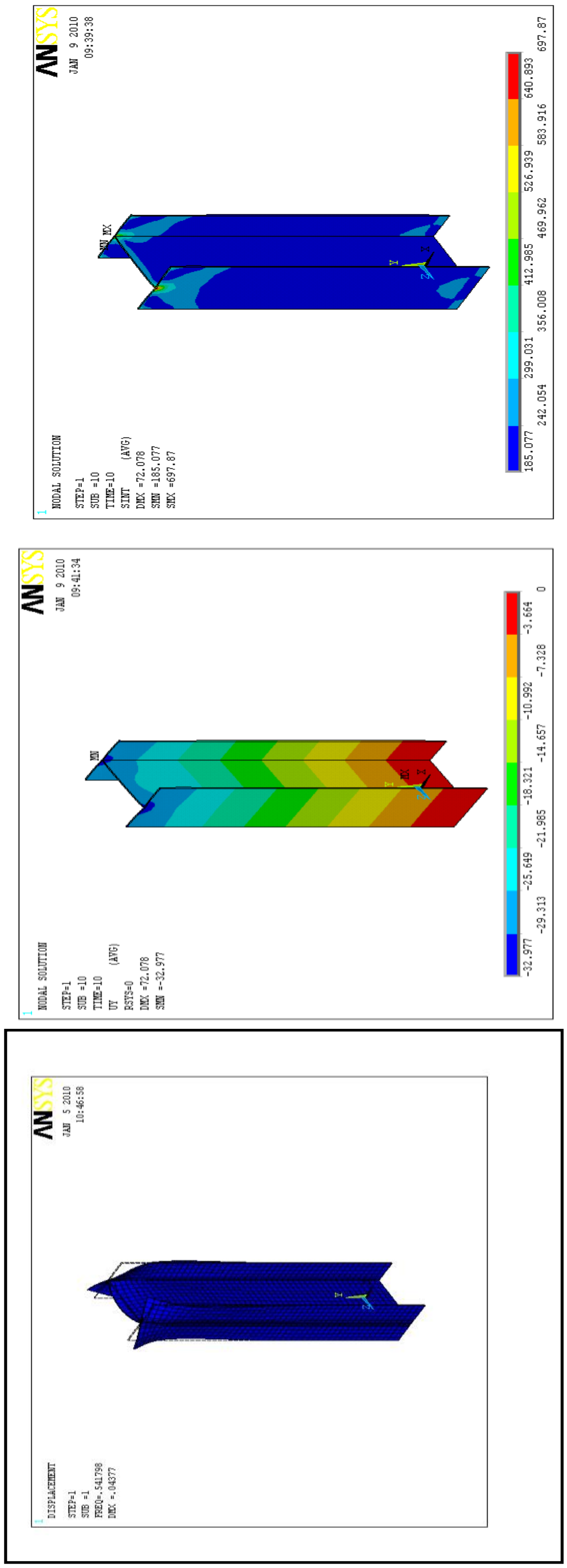

Fig.(16) Distribution of stresses intensity, Axial displacement in Y direction and bulking of NS column by ANSYS-9.

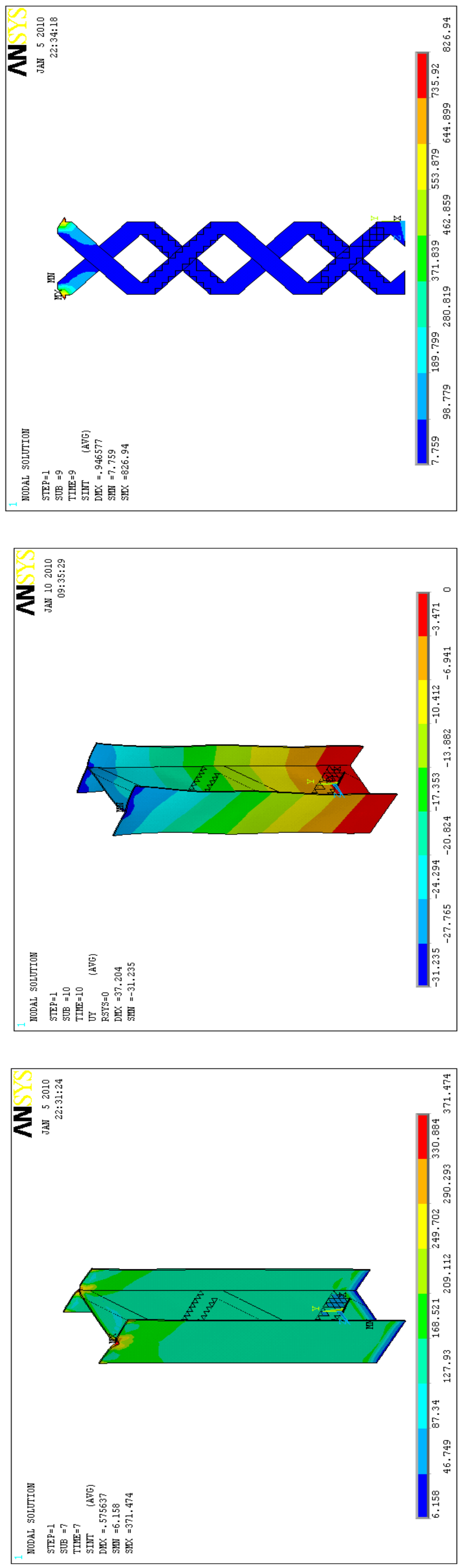

Fig.(17)Distribution of stresses intensity, Axial displacement in Y direction and Distribution of stresses intensity at CFRP of PS1 column by ANSYS-9.

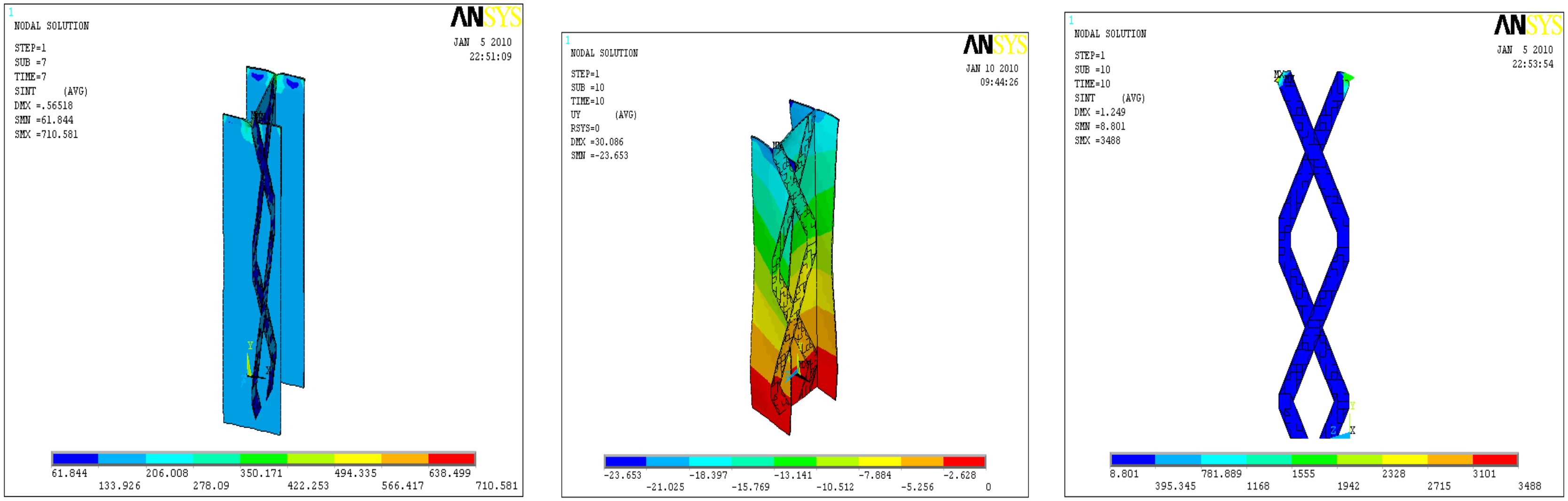

Fig.(18)Distribution of stresses intensity, Axial displacement in Y direction and Distribution of stresses intensity at CFRP of PS2 column by ANSYS-9.

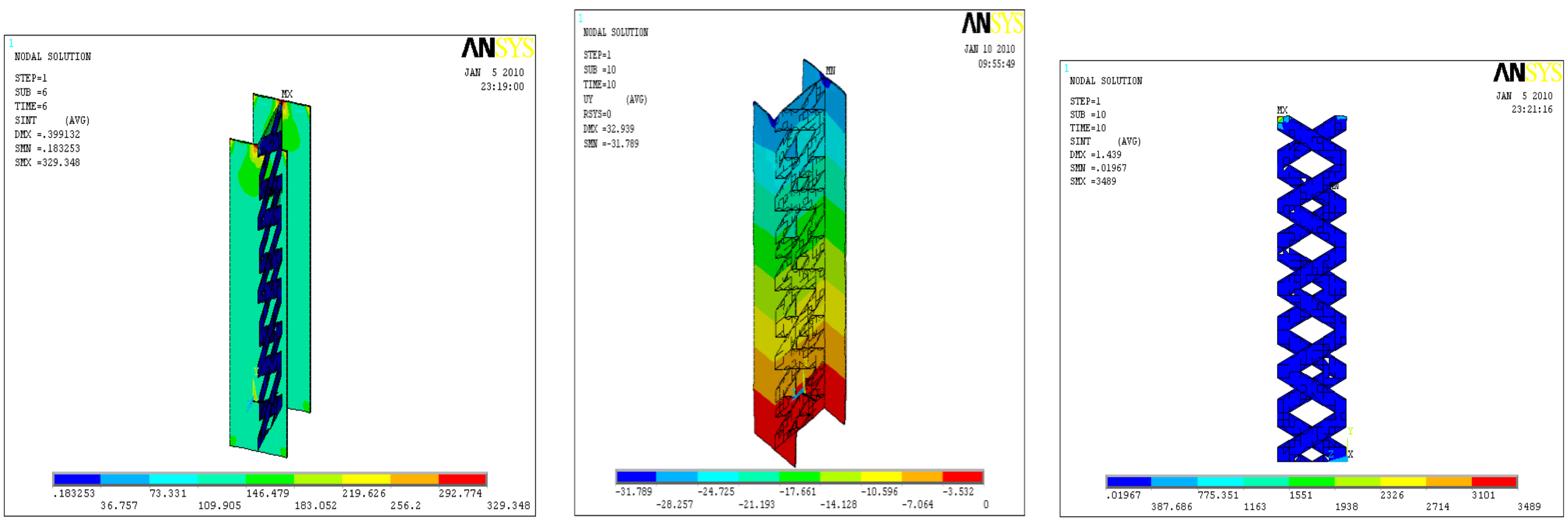

Fig.(19) Distribution of stresses intensity, Axial displacement in Y direction and Distribution of stresses intensity at CFRP of PS3 column by ANSYS-9.

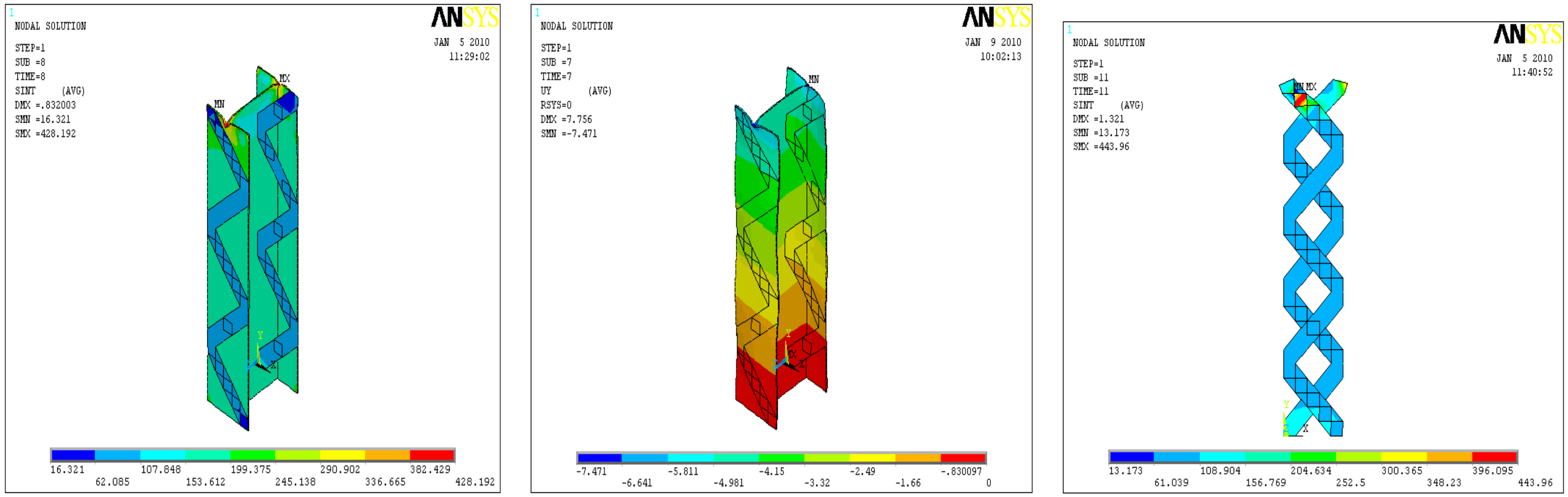

Fig.(20)Distribution of stresses intensity, Axial displacement in Y direction and Distribution of stresses intensity at CFRP of PS4 column by ANSYS-9.

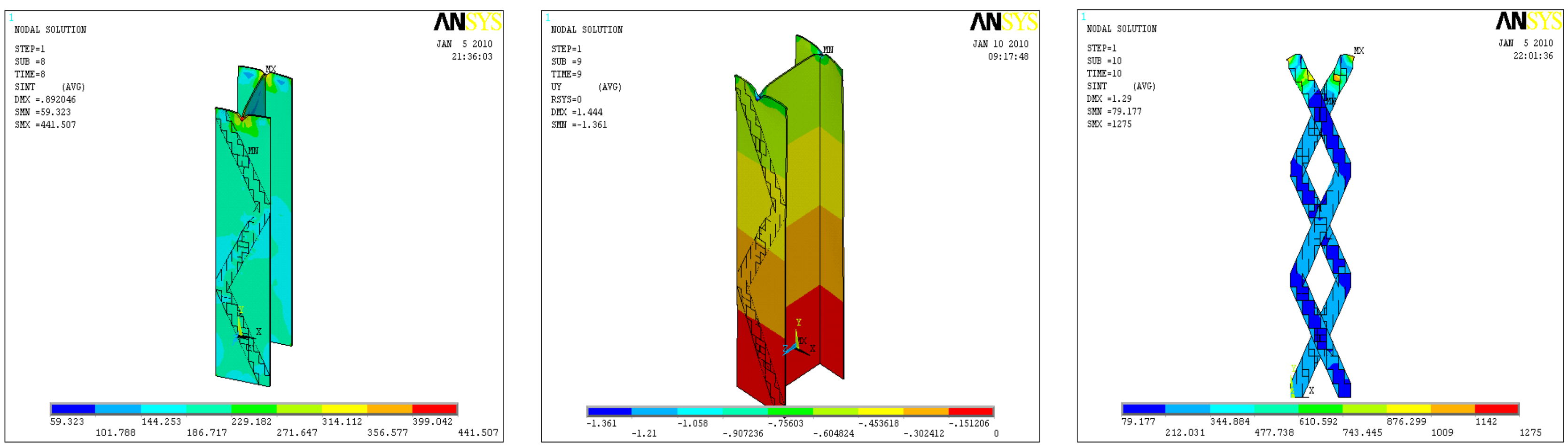

Fig.(21)Distribution of stresses intensity, Axial displacement in Y direction and Distribution of stresses intensity at CFRP of PS5 column by ANSYS-9.

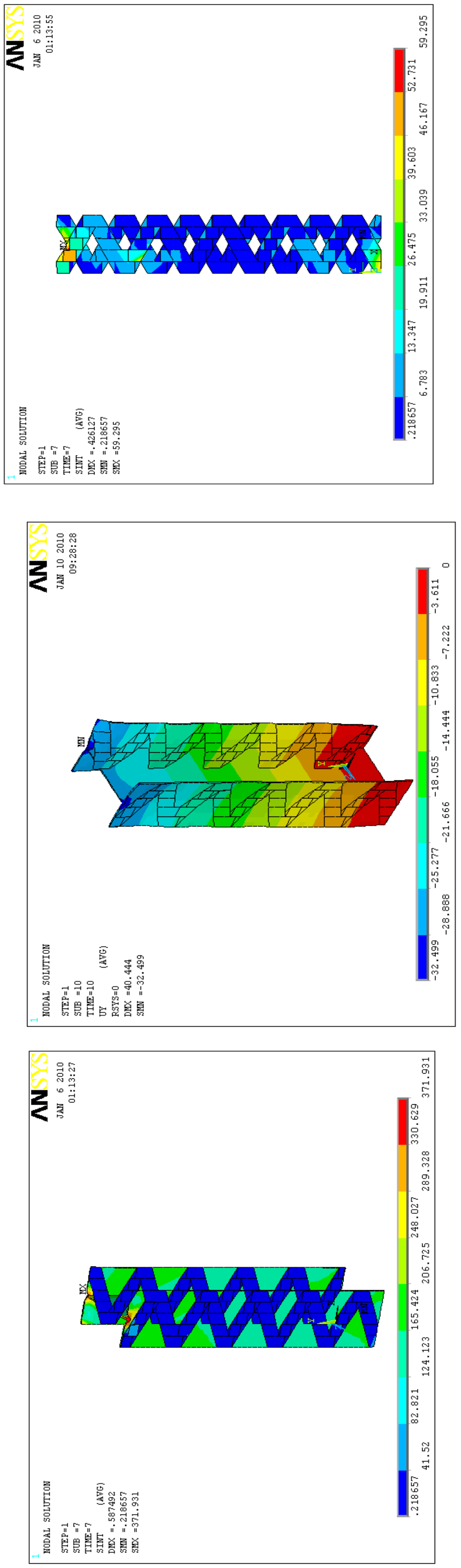

Fig.(22)Distribution of stresses intensity, Axial displacement in Y direction and Distribution of stresses intensity at CFRP of PS6 column by ANSYS-9.

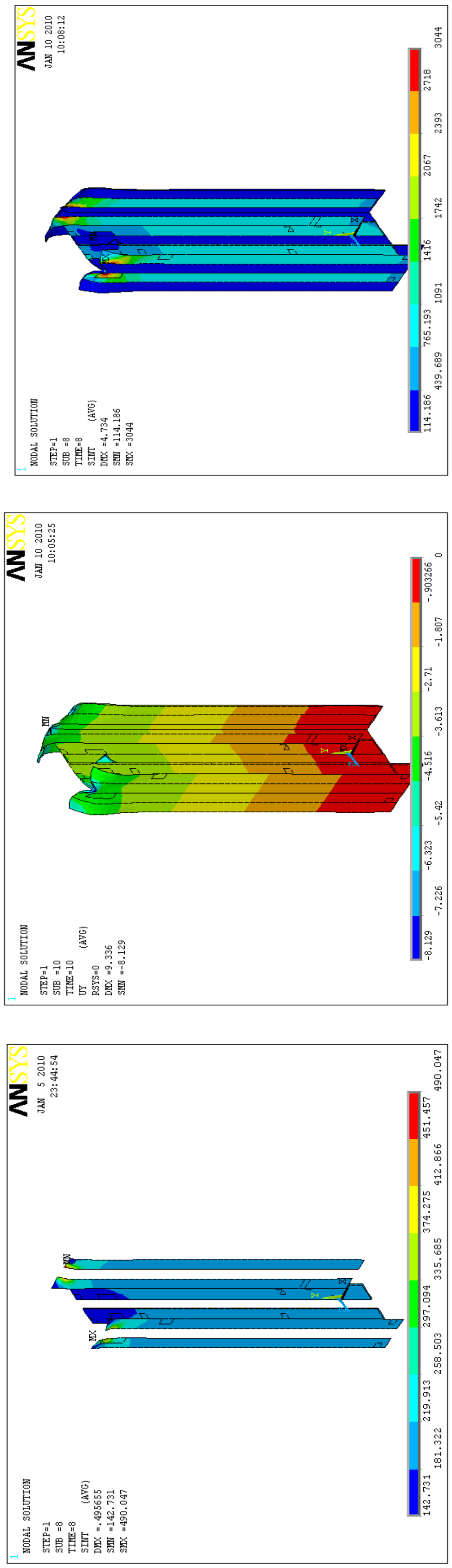

Fig.(23)Distribution of stresses intensity, Axial displacement in Y direction and Distribution of stresses intensity at CFRP of PS7 column by ANSYS-9.

Conclusion:

1) The distribution pattern has a significant effect on the behavior of (I) section steel columns with CFRP, where the pattern of column PS3 given increasing in ultimate capacity more than another columns.
2) The application of CFRP on (I) section steel columns increases the ductility and ultimate compressive load to about 35%.
3) The distribution pattern must be proper with the case of buckling of column which the last depend on the aspect ratio of the column.
4) The anchor system proved with epoxy its effectiveness in carrying the applied force whether the CFRP were bonded or not to the columns.
5) recommend to keep the CFRP working till the column reaches its failure, because in most of the previous researches the CFRPs debonded from the surface and the failure (separation) happened, because of the differences in the stiffness of the three materials (steel, epoxy and CFRP).
6) By use of ANSYS-8 to create the finite element model, the maximum different between experimental results and ANSYS-8 results is 4.8%.

References:

Doi H, et al. Deformation capacity of circular tubular beam-columns reinforced with CFRP subjected to monotonic loading. J Constr Steel 2003;11:431-8[Japan].

Ekiz E. Improving Steel behavior using CFRP warping. Ph.D. Thesis, Department of civil and Environmental Engineering University of Michigan, Ann Arbor, MI,2007.

Hong WS, Zhi MW, Zhi MX, Xing WD. Axial impact behavior and energy absorption efficiency of composite wrapped metal tubes. Int J Impact Eng2000;24:385-401.

Haedir J, Bambach MR, Zhao XL, Grzebieta R. Bending strength of CFRP-strengthened circular hollow steel section. In: Third international conference on FRP composites in civil engineering (CICE) Miami, FL, USA, 2006.

Haedir J, Bambach MR, Zhao XL, Grzebieta R. Behavior of thin-walled CHS beams reinforced by CFRP sheets. Proceeding of the fourth international structural engineering and construction conference (ISEC4), Melbourne, Australia, 2007.

Harries KA., et al. Enhancing stability of structural steel sections using FRP. Thin Walled Struct(2008), doi:10.1016/j.tws.

Jiao H, Zhao XL. CFRP strengthened butt-welded very high strength (VHS) circular steel tubes. Thin-Walled Struct 2004;42(7):963-78.

Teng JG., Hu YM. Behavior of FRP-jacketed circular steel tubes and cylindrical shells under axial compression. Construct Build Mater 2007;21(4):827-38.

Xiao y, He W, Choi K. Confined concrete-filled tubular columns. J Struct Eng, ASCE 2005;131(3):488-97.

Zhao YH, GU W, XU J, Zhang Ht. The strength of concrete-filled CFRP-steel tubes under axial compression. Paper no. 2005-JSC-313, ISOPE Conference, Seoul, June, 2005.

Zhao XL, Fernando ND, AL-Mahaidi R. CFRP strengthened RHS Subjected to transverse end bearing force. Eng Struct 2006;28(11):1555-65.